RELATIONSHIP BETWEEN WALL PRESSURE FLUCTUATIONS AND STREAMWISE VORTICITY IN A TURBULENT BOUNDARY LAYER

Joongnyon Kim
Department of Mechanical Engineering, KAIST
305-701 Taejon, Korea
jnkim@kaist.ac.kr

Jung-Il Choi
Department of Mechanical Engineering, KAIST
305-701 Taejon, Korea
jichoi@kaist.ac.kr

Hyung Jin Sung*
Department of Mechanical Engineering, KAIST
305-701 Taejon, Korea
hjsung@kaist.ac.kr

ABSTRACT

A direct numerical simulation is performed to obtain the correlation between wall pressure fluctuations and streamwise vorticities in a spatially-developing turbulent boundary layer. It is shown that wall pressure fluctuations are related with the upstream streamwise vortices in the buffer region. The maximum correlation occurs with the spanwise displacement from the location of wall pressure fluctuations. The conditionally-averaged vorticity field and the quadrant analysis of Reynolds shear stress indicate that positive wall pressure fluctuations are correlated with the sweep events due to streamwise vortices, while negative wall pressure fluctuations are created beneath the ejection events and vortex cores.

INTRODUCTION

Wall pressure fluctuations, which are a direct measure of the surface excitation force, are closely linked with flow unsteadiness and noise generation in the vicinity of the wall. A knowledge of these quantities is of prime importance in understanding the dynamic behavior of wall turbulent flow. To predict the structural response to turbulent flow and consequent flow-induced noise, much attention has been given to the accurate measurement and calculation of wall pressure fluctuations in the physical and spectral domains. The majority of previous studies have been focused on the investigation of spatial and spectral features of wall pressure fluctuations (Willmarth and Wooldridge, 1962, Schewe, 1983, Choi and Moin, 1990, Farabee and Casarella, 1991).

It is known that the generation of wall pressure fluctuations is governed by the dynamics of velocity fluctuations through a Poisson's equation. A literature survey reveals that the relation of wall pressure fluctuations to near-wall velocity fluctuations has been the subject of both computational and experimental studies (Thomas and Bull, 1983, Kobashi and Ichijo, 1986, Johansson et al., 1987, Kim, 1989, Chang et al., 1999). Thomas and Bull (1983) showed in their experiment that a region of high pressure associated with the sweep motion is due to the passage of inclined near-wall shear layers. By use of an enhanced conditional averaging technique, Johansson et al. (1987) observed that the shear-layer structures in the buffer region are responsible for the generation of large positive wall pressure peaks. This indicates that the wall pressure peaks are linked with the turbulence-producing mechanisms with both ejections and sweeps.

Databases from direct numerical simulations were used to examine the relation be-

*This work was supported by a grant from the National Research Laboratory of the Ministry of Science and Technology, Korea.

tween wall pressure fluctuations and flow structures near the wall. Robinson (1991) found that near-wall shear layers are created when relatively high-speed fluid impacts low-speed fluid lifted by quasi-streamwise vortices. The coherent part of wall pressure fluctuations can be regarded as a footprint connected to streamwise vortices at the buffer region (Kim, 1989). Kim (1989) demonstrated a similarity between spanwise wall pressure gradient $(dp/dz)_w$ and streamwise vorticity at the wall, where the wall pressure is related with the vortical structures in the vicinity of the wall. A region of positive wall pressure are associated with the sweep motions due to streamwise vortices, while negative wall pressure is found to occur beneath vortex core and ejection motions (Bernard et al., 1993). By utilizing this concept, Lee et al. (1998) applied a suboptimal control law for drag reduction. They selected $(dp/dz)_w$ as a sensing parameter and a $16 - 22\%$ reduction in the skin friction was achieved with successful control. Note that the measurement of $(dp/dz)_w$ is much easier in practice by using an array of pressure sensors (Lee and Sung, 1999). These prior studies indicate the need to perform detailed examinations of near-wall flow structures.

The objective of the present study is to obtain a quantitative statistical description of the relation between wall pressure fluctuations and streamwise vortices in turbulent boundary layers. Toward this end, a direct numerical simulation of a turbulent boundary layer with zero pressure gradient is conducted at $Re_\theta = 300$. To generate time-dependent inflow data, turbulence quantities near the exit are rescaled and reintroduced to the inlet of the computational domain (Lund et al., 1998). The main simulation of a developing turbulent boundary layer is then carried out in the range $0 \leq x \leq 200\theta_{in}$, where θ_{in} is the momentum thickness at the inlet. Emphasis is placed on the identification of the relationship between wall pressure fluctuations and streamwise vortices with the long-time averaged statistical description of the correlation. Based on the wealth of DNS data, averaged features of coherent structures are deduced from the conditionally-averaged vorticity field. To secure information on the contributions to the total turbulent energy production, the quadrant analysis of Reynolds shear stress is conducted.

NUMERICAL PROCEDURES

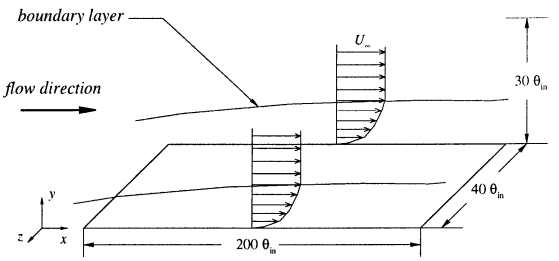

Figure 1: Schematic diagram of the computational domain.

For an incompressible flow, the nondimensional governing equations are

$$\frac{\partial u_i}{\partial t} + \frac{\partial}{\partial x_j} u_i u_j = -\frac{\partial p}{\partial x_i} + \frac{1}{Re}\frac{\partial}{\partial x_j}\frac{\partial u_i}{\partial x_j}, \quad (1)$$

$$\frac{\partial u_i}{\partial x_i} = 0, \quad (2)$$

where x_i are the Cartesian coordinates, u_i are the corresponding velocity components and $i = 1, 2, 3$. All variables are non-dimensionalized by a characteristic length and velocity scale, and Re is the Reynolds number.

The governing equations (1) and (2) are integrated in time by using a fully implicit decoupling method, which has been proposed by Kim et al. (2000). All terms are advanced with the Crank-Nicolson method in time, and they are resolved with the second-order central difference scheme in space. Based on a block LU decomposition, both velocity-pressure decoupling and additional decoupling of the intermediate velocity components are achieved in conjunction with the approximate factorization (Kim et al., 2000). The overall accuracy in time is second-order without any modification of boundary conditions. Since the decoupled momentum equations are solved without iteration, the computational time is reduced significantly.

A schematic diagram of the computational domain is illustrated in Fig. 1. The inlet Reynolds number based on the inlet momentum thickness (θ_0) and free stream velocity (U_∞) is $Re_\theta = 300$. The computational domain has dimensions $200\theta_{in} \times 30\theta_{in} \times 40\theta_{in}$ in the streamwise, wall-normal, and spanwise directions, respectively, where θ_{in} is the momentum thickness at the inlet. The mesh contains $257 \times 65 \times 129$ points in the streamwise, wall-normal, and spanwise directions, respectively. The grid resolution is $\Delta x^+ \cong 12.7$, $\Delta y^+_{min} \cong 0.16$, $\Delta y^+_{max} \cong 22.4$, and $\Delta z^+ \cong 5.3$ in wall units based on the inlet friction velocity.

Uniform grids are deployed in the streamwise and spanwise directions, and a hyperbolic tangent distribution is used for grids in the wall-normal direction. The computational time step used is $\Delta t = 0.3\theta_{in}/U_\infty$ and the total averaging time to obtain the statistics is $1500\theta_{in}/U_\infty$.

Time-dependent turbulent inflow data are provided at the inlet based on the method by Lund et al. (1998). The velocity field from a plane is extracted near the domain exit, modified by the rescaling procedure, and then reintroduced to the inlet of the computational domain. Details regarding the numerical procedures of inflow generation are available in Lund et al. (1998). A convective boundary condition at the exit has the form

$$\frac{\partial u_i}{\partial t} + c\frac{\partial u_i}{\partial x} = 0, \qquad (3)$$

where c is the local bulk velocity. The no-slip boundary condition is imposed at the solid wall, and the boundary conditions on the top surface of the computational domain are

$$u = U_\infty, \quad \frac{\partial v}{\partial y} = 0, \quad \frac{\partial w}{\partial y} = 0. \qquad (4)$$

A periodic boundary condition is applied in the spanwise direction. All the results presented in this paper are obtained at $x_0/\theta_{in} = 100$.

RESULTS AND DISCUSSION

Based on the wealth of numerical data, the correlation $R_{p\omega_x}(\Delta x, y, \Delta z)$ and its corresponding coefficient $R'_{p\omega_x}(\Delta x, y, \Delta z)$ are computed, which are defined as

$$R_{p\omega_x}(\Delta x, y, \Delta z)$$
$$=< p(x_0, 0, z, t)\omega_x(x_0 + \Delta x, y, z + \Delta z, t) >, \quad (5)$$

and

$$R'_{p\omega_x}(\Delta x, y, \Delta z) = \frac{R_{p\omega_x}(\Delta x, y, \Delta z)}{p_{rms}\omega_{xrms}}, \qquad (6)$$

respectively. The bracket denotes an average over the spanwise direction and time. A typical isosurface of the large magnitude of $R'_{p\omega_x}(\Delta x, y, \Delta z)$ is displayed in Fig. 2, which has been obtained by a long-time average. The dark and bright regions indicate positive and negative correlations. The values of 0.12 and -0.12, approximately 20% of the maximum

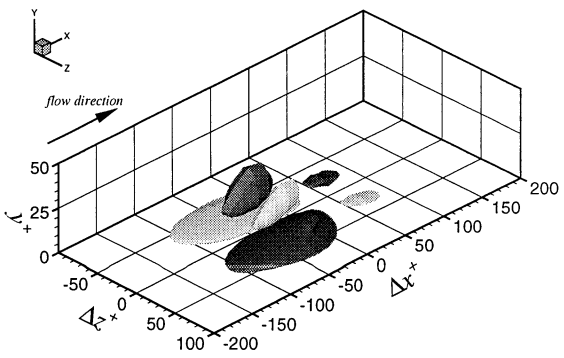

Figure 2: Isosurface plot of correlation between p_w and ω_x in a three-dimensional view.

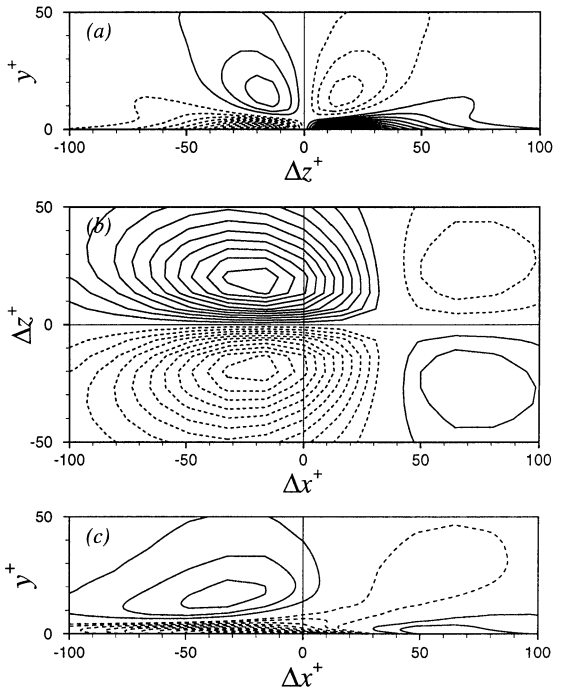

Figure 3: Correlation between p_w and ω_x: (a)contours in the y-z plane at $\Delta x^+ = -20$; (b)contours in the x-z plane at $y^+ = 0$; (c)contours in the x-y plane at $\Delta z^+ = -20$.

magnitude, have been chosen arbitrarily to define the isosurfaces. Figure 2 exhibits a pair of highly correlated structures upstream of the location at which the wall pressure fluctuations are obtained. This is a manifestation of the alternating occurrence of streamwise vortices contributing to high wall pressure fluctuations. The large value of the correlation coefficient at the wall is a kinematic consequence of the interaction between the streamwise vortices above the wall and the no-slip boundary condition. An inspection of Fig. 2 indicates that the high wall pressure fluctuations are associated with the upstream streamwise vortices in the vicinity of the wall.

The contour lines of $R'_{p\omega_x}(\Delta x, y, \Delta z)$ truncated at the planes are exhibited in Fig. 3.

The contour levels are from -0.6 to 0.6 with the increment of 0.05, and the negative correlations are dashed. The contours in the y-z plane are presented in Fig. 3(a), where the maximum correlation coefficient occurs with the spanwise displacement $\Delta z^+ \cong \pm 20$ from the location of wall pressure fluctuations. Note that the spanwise displacement at the wall is also $\Delta z^+ \cong \pm 20$ (Fig. 3(b)), indicating that the strongest correlation coefficients in the vicinity of the wall are observed directly above the locations of those at the wall. Fig. 3(c) discloses that the location of the maximum correlation coefficient moves away from the wall with increasing Δx^+. This confirms the existence of a tilted structure in the vicinity of the wall. The tilted structure was observed by Kravchenko et al. (1993), who examined the relationship between wall skin frictions and streamwise vortices from a direct numerical simulation database of turbulent channel flows. It is seen that the y^+ location of the maximum correlation coefficient increases from $y^+ \cong 15$ at $\Delta x^+ = -50$ to $y^+ \cong 20$ at $\Delta x^+ = -10$, which gives a tilted angle of about 7.13°.

It is recalled that the locations of the positive and negative maxima are at $\Delta x^+ \cong -20$ and $\Delta z^+ \cong \pm 20$ in Fig. 3(b). This is consistent with the result of Jeon et al. (1999), who showed the correlation between the spanwise wall shear-stress (τ_3) and wall pressure fluctuations (p_w). At the wall, since the no-slip boundary condition is applied, the streamwise vorticity can be expressed by the wall-normal gradient of the spanwise velocity $(dw/dy)_w$. For this reason, the shape of contour lines and the locations of maxima in Fig. 3(b) are in close agreement with those of the correlation between τ_3 and p_w.

To examine the structures of streamwise vortices close to the wall, the correlation coefficients at three different spanwise distances Δz^+ are displayed in Fig. 4. The correlation coefficients at $\Delta z^+ \cong -20$ and $\Delta z^+ \cong 20$ have the opposite sign, implying that two streamwise vortices related with the high wall pressure fluctuations are counter-rotating. Accordingly, all the correlations at the position of wall pressure fluctuations ($\Delta z^+ = 0$) are equal to zero (Fig 4.(b)). Note that the correlation coefficient changes sign near $y^+ \cong 5$ in Fig. 4(a). This feature is in good agreement with the streamwise vortex model suggested by Kim et al. (1987), who showed that the streamwise vorticity fluctuations (ω_x) have the local minimum at $y^+ \cong 5$ and the local maximum at

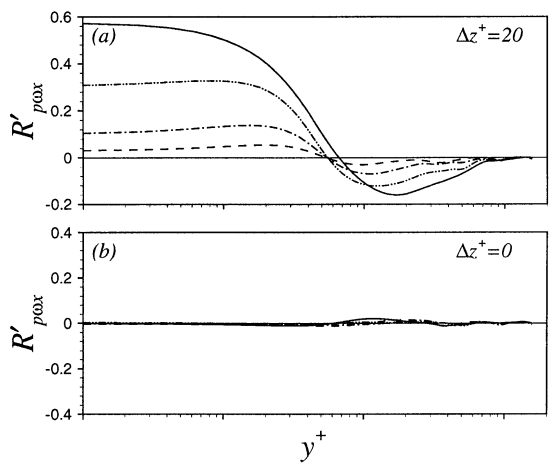

Figure 4: Correlation between p_w and ω_x at various streamwise separations: (a)at $\Delta z^+ = 20$; (b)at $\Delta z^+ = 0$.

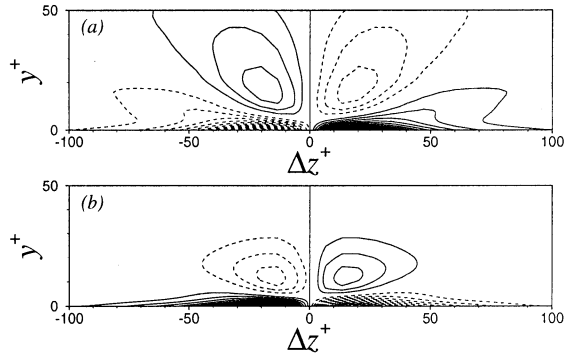

Figure 5: Conditionally-averaged streamwise vorticity field: (a)$p_w > 2p_{rms}$; (b)$p_w < -2p_{rms}$.

$y^+ \cong 20$. They reasoned that the location of the local maximum corresponds to the average location of the center of streamwise vortices, and that the local minimum corresponds to the existence of the streamwise vorticity with opposite sign created at the wall.

As seen in the correlation between wall pressure fluctuations and near-wall streamwise vorticities, high wall pressure fluctuations are associated with the streamwise vortices in the vicinity of the wall. In order to deduce an averaged features of coherent structures, the conditionally-averaged streamwise vorticity fields are calculated for various threshold levels of wall pressure fluctuations. The streamwise vorticities near the position of high wall pressure fluctuations are averaged for positive and negative pressures, respectively. The conditional averages of streamwise vorticity are constructed satisfying the condition

$$p_w \geq k p_{rms}, \tag{7}$$

for the positive wall pressure fluctuations, and

$$p_w \leq -k p_{rms}, \tag{8}$$

for the negative wall pressure fluctuations. Here, k is a threshold value. The results in the case of $k = 2$ are exhibited in Fig. 5. The contours of the conditional averages are truncated at $\Delta x^+ \cong -20$ in the y-z plane. It is evident in Fig. 5(a) that the region of high positive wall pressure is linked with the inward motion of fluid particles due to the streamwise vortices above the wall. On the contrary, the high negative wall pressure fluctuations are found to occur beneath the outward motion of fluids in the vicinity of the wall (Fig. 5(b)). Note that the y^+ location of the local maximum of the vorticity for the negative wall pressure fluctuations is closer to the wall than that for the positive wall pressure fluctuations. This suggests that the streamwise vortices associated with negative wall pressure fluctuations are closer to the wall. Comparison of the conditionally-averaged results for different threshold values reveals that the shapes and sizes of vortices are almost the same, while the strengths for the case of lower threshold values are much weaker than those of higher threshold values.

In order to deduce the generation of wall pressure fluctuations contributing to the production of turbulent energy, the quadrant analysis of the Reynolds shear stress is performed for various threshold levels of wall pressure fluctuations. Since most of the turbulent energy production comes from $-\overline{u'v'}\partial U/\partial y$, the analysis divides the Reynolds shear stress into four categories according to the signs of u' and v'. The first quadrant ($u' > 0$ and $v' > 0$) contains outward motion of high-speed fluid; the second quadrant ($u' < 0$ and $v' > 0$) contains the motion associated with ejections of low-speed fluid away from the wall; the third quadrant ($u' < 0$ and $v' < 0$) contains inward motion of low-speed fluid; and the fourth quadrant ($u' > 0$ and $v' < 0$) contains the motion associated with sweeps of an inrush of high-speed fluid (Kim et al., 1987). The second and fourth quadrant events contribute to positive turbulent energy production, and the first and third quadrant events contribute to negative production.

The Reynolds shear stress from each quadrant is averaged satisfying the condition (7) and (8). The average over time is directly constructed above the location of the wall pressure fluctuations. The contributions to the Reynolds shear stress from each quadrant, normalized by the free stream velocity, are shown in Fig. 6. The results according to the sign of the wall pressure fluctuations, i.e. in the case of $k = 0$, are exhibited in Fig. 6. It is found in Fig. 6(a) that the fourth quadrant events associated with positive wall pressure fluctuations have larger contributions to the production of turbulent energy near the wall region. On the contrary, the second quadrant events are dominant when negative wall pressure fluctuations are generated (Fig. 6(b)). This suggests that the sweep motions due to streamwise vortices are responsible for the generation of positive wall pressure fluctuations, while negative wall pressure fluctuations are created beneath the ejection motions. As the threshold value increases, the resulting prevalence of Reynolds-shear-stress-producing events is intensified. In the case of $k = 1$, it is seen that the contributions of the dominant quadrant events to the production of turbulent energy are larger than those in the case of $k = 0$.

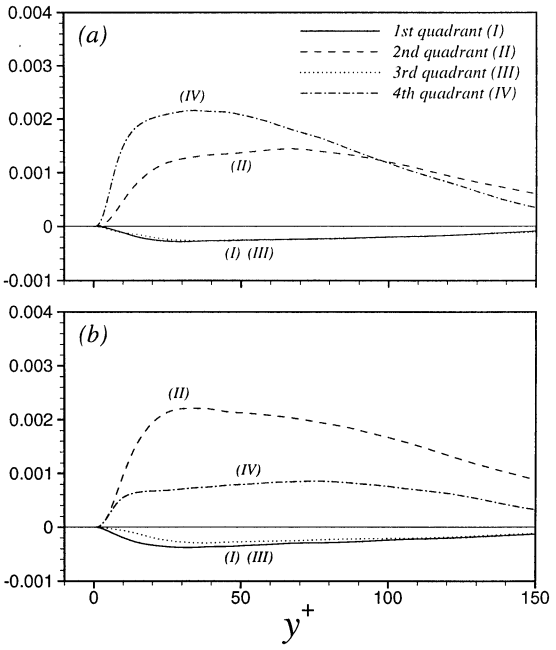

Figure 6: Reynolds shear stress $-\overline{u'v'}$ from each quadrant normalized by free stream velocity: (a)$p_w > 0$; (b)$p_w < 0$.

CONCLUSION

A detailed numerical analysis has been performed to delineate the relationship between wall pressure fluctuations and near-wall streamwise vortices in a turbulent boundary layer with zero pressure gradient. The statistical descriptions of the correlation between wall pressure fluctuations and streamwise vorticity were obtained by performing a direct numerical simulation of a spatially-developing

turbulent boundary layer at $Re_\theta = 300$. It was found that the generation of wall pressure fluctuations is associated with the streamwise vortices in the vicinity of the wall. The streamwise vortices are tilted from the wall in the streamwise direction and the tilted angle is about 7.13°. The maximum correlation occurs upstream and with the spanwise displacement $\Delta z^+ \cong \pm 20$ from the location of wall pressure fluctuations. The average location of the streamwise vortices is consistent with the streamwise vortex model suggested by Kim et al. (1987). A region of positive wall pressure fluctuations is linked with the sweep motions due to the streamwise vortices in the buffer region. On the contrary, the negative wall pressure fluctuations are found beneath the ejection motions. These Reynolds-shear-stress-producing events associated with the streamwise vortices contribute mostly to the production of turbulent energy.

REFERENCES

Bernard, P. S., Thomas, J. M., and Handler, R. A., 1993, "Vortex dynamics and the production of Reynolds stress", *J. Fluid Mech.*, Vol. 253, pp. 385-419.

Chang, P. A., Piomelli, U., and Blake, W. K., 1999, "Relationship between wall pressure and velocity field sources", *Phys. Fluids*, Vol. 11, pp. 3434-3448.

Choi, H., and Moin, P., 1990, "On the space-time characteristics of wall-pressure fluctuations", *Phys. Fluids*, Vol. A2(8), pp. 1450-1460.

Farabee, T. M., and Casarella, M. J., 1991, "Spectral feature of wall pressure fluctuations beneath turbulent boundary layer", *Phys. Fluids*, Vol. A3, pp. 2410-2420.

Jeon, S., Choi, H., Yoo, J. Y., and Moin, P., 1999, "Space-time characteristics of the wall shear-stress fluctuations in a low-Reynolds-number channel flow", *Phys. Fluids*, Vol. 11 (1), pp. 3084-3094.

Johansson, A. V., Her, J. -Y., and Haritonidis, J. H., 1987, "On the generation of high-amplitude wall-pressure peaks in turbulent boudnary layers and spots", *J. Fluid Mech.*, Vol. 175, pp. 119-142.

Kim, J., Moin, P., and Moser, R., 1987, "Turbulence statistics in fully developed channel flow at low Reynolds number", *J. Fluid Mech.*, Vol. 177, pp. 133-166.

Kim, J., 1989, "On the structure of pressure fluctuations in simulated turbulent channel flow", *J. Fluid Mech.*, Vol. 205, pp. 421-451.

Kim, K., Baek, S. -J., and Sung, H. J., 2000, "An implicit velocity decoupling procedure for the incompressible Navier-Stokes equations", *Int. J. Numerical Methods in Fluids*, submitted.

Kobashi, Y., and Ichijo, M., 1986, "Wall pressure and its relation to turbulent structure of a boundary layer", *Exp. Fluids*, Vol. 4, pp. 49-55.

Kravchenko, A. G., Choi, H., and Moin, P., 1993, "On the relation of near-wall streamwise vortices to wall skin friction in turbulent boundary layers", *Phys. Fluids*, Vol. A 5 (12), pp. 3307-3309.

Lee, C., Kim, J., and Choi, H., 1998, "Suboptimal control of turbulent channel flow for drag reduction", *J. Fluid Mech.*, Vol. 358, pp. 245-258.

Lee, I., and Sung, H. J., 1999, "Development of an array of pressure sensors with PVDF film", *Exp. Fluids*, Vol. 26, pp. 27-35.

Lund, T. S., Wu, X., and Squires, K. D., 1998, "Generation of turbulent inflow data for spatially-developing boundary layer simulations", *J. Comput. Phys.*, Vol. 140, pp. 233-258.

Robinson, S. K., 1991, "Kinematics of turbulent boundary layer structure", Ph.D. dissertation. Stanford Univ., Stanford.

Schewe, G., 1983, "On the structure and resolution of wall-pressure fluctuations associated with turbulent boundary-layer flow", *J. Fluid Mech.*, Vol. 134, pp. 311-328.

Thomas, A., and Bull, M., 1983, "On the role of wall pressure fluctuations in deterministic motions in the turbulent boundary layer", *J. Fluid Mech.*, Vol. 128, pp. 283-322.

Willmarth, W. W., and Wooldridge, C. E., 1962, "Measurement of the fluctuating pressure at the wall beneath a thick boundary layer", *J. Fluid Mech.*, Vol. 14, pp. 187-210.